LOCATING WATER POLLUTION AND SHORE DISCHARGES IN COASTAL ZONE AND INLAND WATERS WITH FLS LIDAR

Sergey Babichenko[1], Alexander Dudelzak[2], Jüri Lapimaa[3], Alexei Lisin[3], Larisa Poryvkina[3] and Alexandre Vorobiev[1]

1. Laser Diagnostic Instruments International Inc., 146 Colonnade Road South, Unit 1, Ottawa, Ontario, Canada K2E 7Y1; info(at)ldi3.com
2. Canadian Space Agency, 6767 rue de l'Aeroport, Saint Hubert, Quebec, J3Y 8Y9, Canada; alex.dudelzak(at)space.gc.ca
3. AS Laser Diagnostic Instruments, 113A Kadaka str., 12915 Tallinn, Estonia; ldi(at)ldi.ee

ABSTRACT

The paper reviews results of field studies and pilot projects with airborne Fluorescent Laser Spectrometers (FLS-lidars) carried out in 2003-2004 in sea and lake waters as well as watersheds. Those studies were aimed at locating areas with water quality deviations from normal state due to municipal and agriculture discharges and chemical pollution. The studies were conducted in Ontario and Estonia based on airborne surveys, corroborated by simultaneous collection and laboratory analysis of flight-path ground samples. The goal of these projects was to provide a comparative study, using a combination of traditional sampling with following laboratory analysis and Laser Induced Fluorescence (LIF) and Spectral Fluorescence Signature (SFS) techniques. Spatial changes in the composition of dissolved organic matter, indicating possible agricultural run-off or sewage-related discharge, were clearly tracked, and oil pollutions in water were detected and quantified. A combination of LIF and SFS technologies was validated as a valuable tool for near real-time environmental assessment.

Further developments of FLS-lidar resulted in an increase of sensing distance, spatial resolution and implementation of a laser beam scanning system capable of providing a swath on the underlying surface. The advanced model FLS-AM based on a new XeCl excimer laser (150 mJ / 150 Hz), a hyper-spectral detector (Intensified CCD) and a self-adjusted telescope coupled with a scanner operates at altitudes of up to 500 m and enables the scanned strip to be sensed at a width equal to 20% of the flight altitude. The results of field tests confirmed a considerable improvement of the operational characteristics of FLS-lidar. Its operational use in multi-tiered environmental monitoring applications is discussed.

Keywords: Laser Induced Fluorescence, Spectral Fluorescent Signatures, oil pollution.

INTRODUCTION

Laser remote sensing has been proved to be an efficient and often the only tool in many environmental applications, capable of providing quantitative, spatially resolved, real-time data of oil pollution (1,2,3), eutrophication (4), and estimation of biomass in natural waters (5) and on the ground (6) etc. Previously reported developments and experiments with the FLS-lidar (7) have confirmed that the use of hyper-spectral detectors in LIF applications delivers additional analytical capabilities for laser remote sensing. Recording a comprehensive LIF spectrum at every laser pulse with following analysis of the spectral patterns allows an expert system to be built for qualitative and quantitative analysis of surveyed water bodies and land surfaces.

Recently completed airborne surveys with FLS-AU lidar for water quality monitoring (Dec 2003, Ontario, in cooperation with Environment Canada and Ontario Conservation Authorities) (8), location of land pollution (Apr 2004, Estonia, in the frame of the Tallinn – Helsinki EUREGIO project) and oil spill detection (May 2004, France, in cooperation with SAS ActiMAr in the frame of the DEPOL04 experiment (9) have defined the directions of further developments aimed at improving the operational parameters of the FLS-lidar.

An increasing sensing distance up to at least 500 m has revealed to be a necessary requirement for combining LIF measurements with other sensors. Higher spatial resolution – better than 10 m – was considered essential for land observation. Scanning the laser beam across the flight path providing the swath on the underlying surface was defined as of high priority for both water and land applications, especially for oil spill detection and mapping, monitoring of watersheds and main lines (oil pipelines, railways, roads etc.).

Building a robust expert system for real-time operation, simple enough to minimize processing and reporting time in flight, has manifested as a critical issue for operational use of the FLS-lidar. It has also been confirmed that the additional flexibility of unattended lidar operation is provided by a video- and navigation/targeting system integrated into the lidar set-up. These requirements have been realised in developing a new model in the FLS-series – the FLS-AM lidar. This lidar has been successfully tested in airborne experiments in Estonia and is in preparation for operational use.

The present paper describes the application of FLS-AU and FLS-AM lidars in a Multi-tier Model for Integrated Environmental Assessment based on the airborne surveys completed in 2003-2004.

DEVICES AND METHODS

A combination of airborne LIF, on-site SFS and laboratory technologies has been used for environmental assessment in the present studies.

Multi-tier Model for Integrated Environmental Assessment

The primary concept is to start with a rapid, large-scale assessment of an entire region, identifying stressed environments and zones of high interest, which can then be studied in detail utilising on-site and time-consuming methods (Figure 1). In this model, the lidar serves at the 1st tier and produces an extensive data set. Real-time or post-processing are used to locate the points of interest, e.g. water pollution or other environmental stress, and to direct the ground sampling activity.

In a 2nd tier, the on-site analyses of water or ground samples can be carried out applying the SFS technique. As the measuring principle is based on induced fluorescence and optical absorption, the SFS is easy to use for quantitative calibration of lidar data. Due to its analytical capability of identifying and quantifying many organic compounds in different environments the SFS technique serves also to select the samples for further detailed laboratory tests. Finally, in the 3rd tier, a detailed laboratory analysis of the selected samples is carried out yielding a high percentage of actionable results.

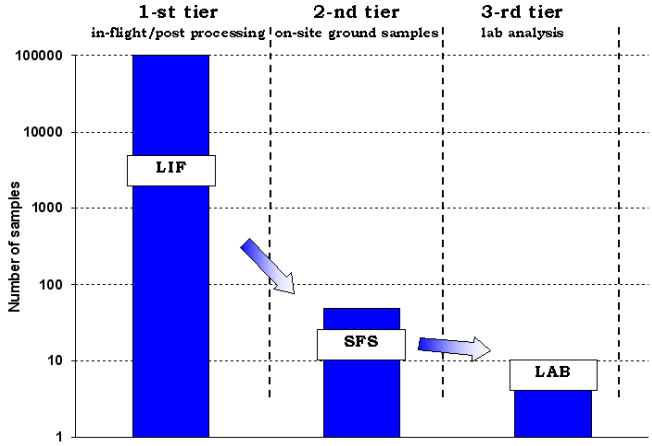

Figure 1: Multi-tier model for environmental assessment.

This model decreases the number of samples through the tiers substantially with an increase in information value of every sample at the last stage. Integration and cross-referencing of the collected data at all three stages provides valuable calibration and statistical benefits. It appears to be very promising for the optimization of environmental assessment activities by increasing the percentage of useful data (which can be constructively acted upon) and streamlining the allocation of human and technical resources.

FLS-Lidar

The schematics of FLS-lidars are based on the excimer laser as a main light source and a hyperspectral detector (gated intensified CCD camera coupled with flat-field polychromator). Read-out of the fluorescence spectrum per laser pulse allows a detailed analysis of the spectral shape of the LIF spectrum. The lidar is fully controlled by operational software in an unattended mode. Every measured LIF spectrum is accompanied by GPS coordinates and time stamp, and stored in the database.

The FLS-AU lidar was built as a down-looking airborne system with separate beam expander and receiving telescope. A UV beam expander is used to decrease the beam divergence and to fulfill the eye safety requirements. At the maximum pulse repetition rate of 20 Hz the FLS-AU lidar provides a typical spatial ground resolution of 6 m (at 200 km/h flight speed). Moderate weight and power consumption enables the system to be operated on board of small aircraft at altitudes of up to 300 m.

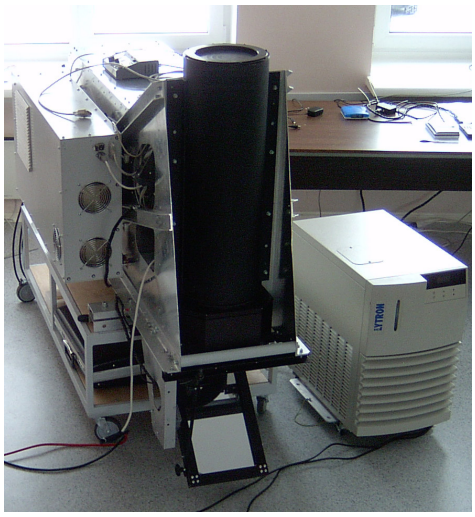

Figure 2: The FLS-AM lidar.

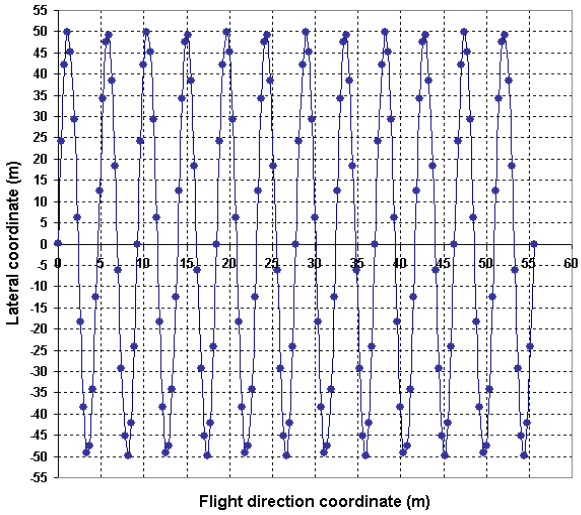

Figure 3: Laser footprints on the ground.

The FLS-AM lidar (Figure 2) was built as a down-looking-and-scanning airborne system with self-adjusted telescope serving simultaneously as a transmitting and receiving system. A new model of ruggedized excimer laser (150mJ / 150Hz) serves as a sensing source. The scanning of expanded laser beams across the flight trajectory enables the ground level corridor to be observed at a width of 20% of the flight altitude (Figure 3).

The lidar has an integrated targeting video camera-based system. It has two video outputs, one for the pilot screen to target the aircraft, and another one to store video frames of the underlying surface. Full lidar control is provided by an integrated microcontroller according to the operation set-up stored in advance. Lidar control and data visualization are done also in real-time mode *via* an operator console. LIF spectra accompanied by GPS position and video frame are stored in the database using the Microsoft® Jet Database engine.

Table 1: Comparative table of FLS-AU and FLS-AM parameters.

	FLS-A(U)	**FLS-A(M)**
Sensing distance	50 - 300 m	50 - 500 m
Operation mode	Down-looking	Scanning across the flight path Scanned width: 1/5 of the altitude
Laser source	Excimer, 308 nm, 90 mJ / 20 Hz	Excimer, 308 nm, 150 mJ / 150 Hz Dye-laser, 360 nm, 460 nm
Detector type	Gated Hyperspectral, 500 channels	
Spectral range	300 - 550 nm	Tunable 250 nm spectral window
Power consumption	1.2 kVA, 28 DC	6 kVA, 28 DC
Dimensions (L × W × H)	1569 × 614 × 795 mm^3	1660 × 685 × 1004 mm^3
Full system weight	180 kg	375 kg

On-line and retrospective data processing

Real-time LIF data processing is a challenging task due to the intensive data flow from the lidar to the processing computer. At an FLS-AM sampling rate of 150 Hz and a detector frame of 500 channels, an array of 75,000 spectral intensity data per second is transferred to the control computer and processed. In fact, the amount of data is twice as high, as the background spectral signal is also recorded between the laser pulses and subtracted from the LIF spectrum to exclude the influence of glint reflections and ambient light recorded during the detector gate pulse.

While retrospective data processing can be done based on sophisticated algorithms, the Real-time operating expert system has to be robust and simple enough to minimize the processing time in flight. The intensity of water Raman scattering when observing a fixed water layer serves as an indicator of water transparency. Simple algorithms of normalizing LIF intensities by water Raman scattering are quite effective to measure spatial trends of Dissolved Organic Matter (DOM) and chemical pollution in open waters. The analysis becomes more challenging when observing shallow waters or terrestrial targets due to a higher variability of LIF spectra as compared with open water basins.

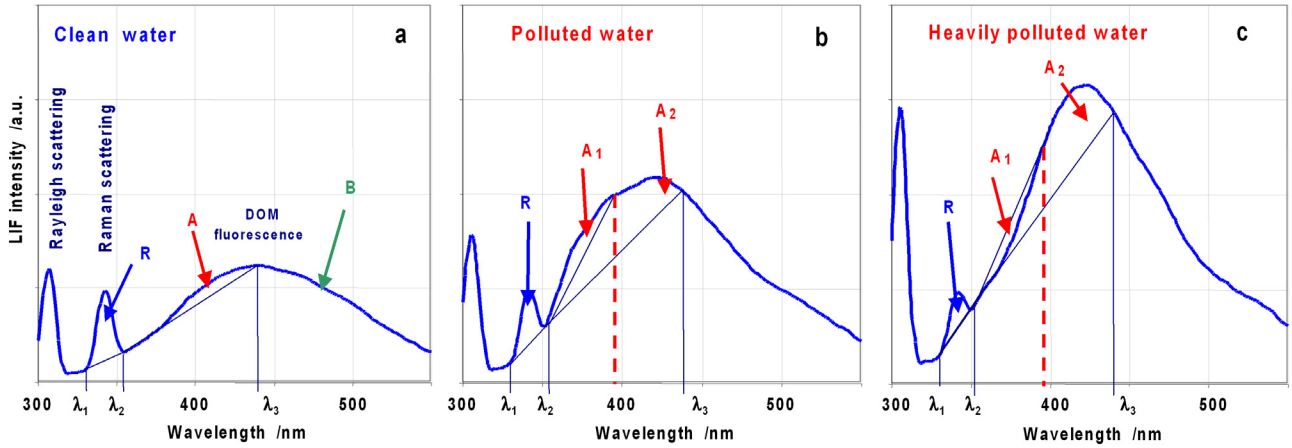

Figure 4: Schematics of LIF spectrum processing based on spectral asymmetry.

Figure 4 shows one of the robust schematics of water LIF spectra processing in real time for detection of oil pollution in water. It is based on the simplified analysis of variations in the shape of LIF spectra (asymmetry) due to different water types and pollutions (7). Post-processing typically requires decomposition of the measured LIF spectra by using a pre-compiled spectral library of different underlying surfaces and pollutants in combination with SFS and laboratory analysis of ground samples (10). The correlation of results between these two algorithms was found at a level of 0.78 based on a set of 6,000 LIF spectra processed. It confirms that the model can be used for in-flight reporting the points of interest.

The integral spectral intensities *R*, *A*, *B* inside the marked spectral ranges for clean water spectrum (Figure 4a) serve as references. The first spectral range is defined by the inflections of the water Raman signal (wavelengths λ_1, λ_2), and *R* value is produced as the integral of the spectral intensities above the linear slope between λ_1 and λ_2. The second spectral range is selected between λ_2 and the wavelength of maximal intensity of DOM fluorescence (λ_3), and *A* is calculated by spectral intensity integration above the slope between λ_2, and λ_3. To detect pollution in water the second spectral range (λ_2, λ_3) is split into two sub-ranges of equal spectral width (red dashed line in Figure 4) and separate integral intensities A_1 and A_2 are calculated according to the algorithm described above. When $A_1>0$ and $A_2>A$ (Figure 4b), the expert system classifies the water as polluted, and the linear calibration of fluorescence by oil concentration is applied. When $A_1<0$ and $A_2>A$ (Figure 4c), it indicates optically dense water (heavily polluted), and a calibration corrected with spectral absorption has to be used. The *B* value (Figure 4a) can be applied to detect changes in DOM composition in the area of observation on condition that $A_2 = A$. An increasing *B* value as compared to clean water often indicates a higher ratio of terrestrial DOM fractions typically reflecting shore discharge (11).

Such a simplified algorithm is mainly used for in-flight detection of pollution spots and trends recording. The findings of the expert system can serve to specify the areas where ground sampling is required for further post-processing and calibration of remote sensing data.

Spectral Fluorescent Signatures (SFS)

The concept of Spectral Fluorescent Signatures (SFS) has added to analytical lidar sensing the capability of detecting and identifying trace substances in a variety of targets in the presence of other, background matter responding to optical excitation with overlapping signals. The SFS is recorded as a multi-dimensional matrix of intensity and spectral parameters. Various organic compounds are manifested in such a matrix as specific structural singularities representing the SFS. The SFS topology (spectral "fingerprint") serves as substance identifier, while the fluorescence intensity is used as a measure of substance quantity. With the SFS technique, the task of biochemical analysis becomes an issue of recognition and de-convolution of spectral images (12).

Figure 5 shows typical SFS of the water samples collected in the study area measured with an SFS analyzer Fluo-Imager®. The colour plots represent the levels of fluorescence intensity (from blue to white) in coordinates of excitation and emission wavelength, the number displays the maximal SFS intensity marked by black dots. The differences in topography are easily noticeable. The SFS of clean lake water (Figure 5a) contains a Raman scattering line along the left side of the plot and the wide spectral structure of DOM. The SFS of polluted water has additional spectral signals in the near-UV area (Figure 5b), while the increase of terrestrial fractions causes the red shift of the DOM spectral structure (Figure 5c).

The software expert system based on a pre-compiled calibrated library of SFS of organic compounds provides qualitative (identification) and quantitative analysis of water contamination (13). The SFS technique provides an effective way of remote data calibration due to its analytical capability and similarity of the measuring principle with LIF. Additional laboratory analysis is typically required if some unknown compounds in the water are diagnosed or the expert system cannot find the best fit in the library. The SFS technique applied at the second tier of environmental assessment can significantly reduce the final number of laboratory analyses (Figure 1).

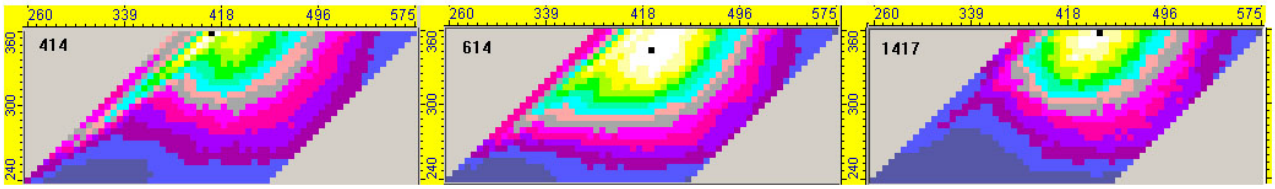

Figure 5: The SFSs of water samples in the Ontario region: (a) clean water of the Lake Ontario; (b) oil-polluted water in Hamilton Harbour; (c) Shore run-off in the Grand River.

RESULTS

In December 2003, Laser Diagnostic Instruments (LDI) had completed an extensive airborne survey of surface water-quality monitoring and identification of contamination sources in Ontario, Canada with the FLS-AU lidar (see the map in Figure 6 for reference). Territories observed with 30 m spatial resolution in average included the Lake Simcoe; the Lake Ontario, the Lake Erie, the Lake Huron, the Welland canal, the Grand River; the Maitland River; the Saugeen River etc. Near-simultaneous sampling of ground water was carried out along the Grand River, the Maitland River, and in Hamilton Harbour. In addition to the water systems mentioned above, an aerial survey of the Gobles oil fields and of Six Nations Reserve lands was performed for the purpose of gathering data on soil conditions.

The surveillance was performed on board of a Rockwell Aerocommander aircraft at altitudes of 100 – 150 m according to the multi-tier model. Qualitative real-time airborne LIF assessment of pollution patterns and water characteristics and their geo-referencing were done in-flight. An accumulation mode (3 laser pulses) was used to record every LIF spectrum. The SFS processing of ground samples was carried out after the flight for cross-correlation of LIF and SFS data. A detailed post-flight laboratory analysis of selected ground samples has been completed for quantita-

tive calibration of LIF data. As a result of the survey, water properties and pollution patterns have been characterized for the covered territory.

Figure 6: Flight track in Ontario (green line).

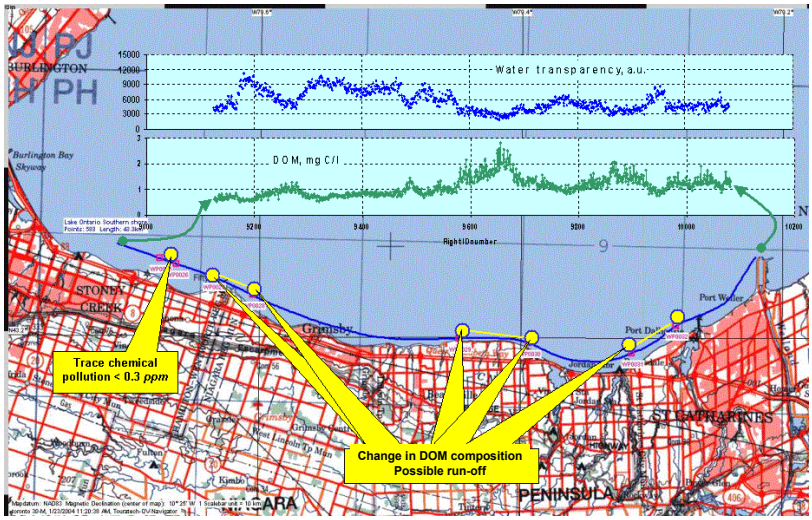

Figure 7: South shore of Lake Ontario with flight track (blue line), water transparency (blue profile, abs. values of ADC readings), DOM given by DOC (green profile), and findings.

The recorded database consisted of about 800,000 LIF spectra with more than 70 findings in water (deviations of water quality) and more than 100 findings on the ground. Among them, 19 water samples were selected for laboratory processing at the environmental laboratory of Ontario Ministry of Environment to calibrate SFS and LIF data. High correlation (r^2=*0.95*) was evident for Dissolved Organic Carbon (DOC) and Total Organic Carbon (TOC) content defined by SFS and standard MOE laboratory analysis.

Figure 7 demonstrates LIF data trends of DOM, and of water transparency represented by water Raman scattering measured in-flight along the Lake Ontario shore. The marked points were selected by the expert system as deviating from normal stage and corresponding to potential shore run-off and river water discharge. Figure 8 shows the flight segment along the shore of Lake Ontario with readings of low-level oil pollution in the Toronto port area and Hamilton Harbour. According to cross-correlation with SFS data of water samples the minimal detectable concentration of oil pollution by FLS-AU lidar was 0.3 *ppm*.

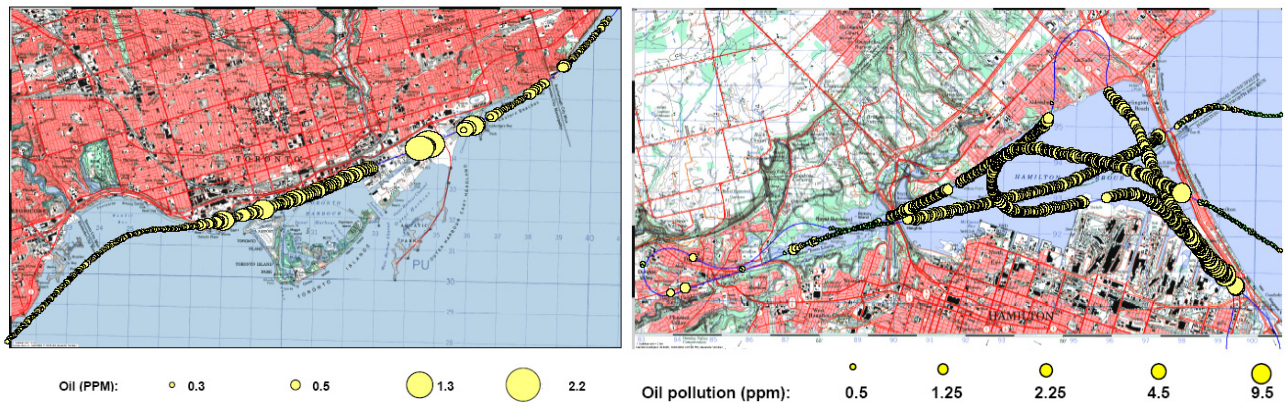

Figure 8: Toronto Port area (left) and Hamilton Harbour area (right), calibrated oil pollution readings.

Some examples of findings are listed below. A noticeable contrast between Hamilton Harbour water and the Lake Ontario water was registered due to significantly higher DOM/DOC content (up to 10 mg C/l) and multiple occurrences of different oil pollutions (including oil films on the water surface) in harbour waters. SFS analysis of water samples has revealed light oils (up to 1.7 *ppm*), residual oils (up to 5.2 *ppm*) and waste oil products (up to 3.2 *ppm*). Strong gradients of water

transparency and DOM (from 1.8 mg C/l to 12 mg C/l) were recorded in the Lower Grand River upon entry into the river from the Lake Erie and up to the town Brandfort. Chemical pollution sites, including oil pollution, were located in the Maitland River. Multiple suspect areas with DOC-rich run-off were detected in the Welland canal.

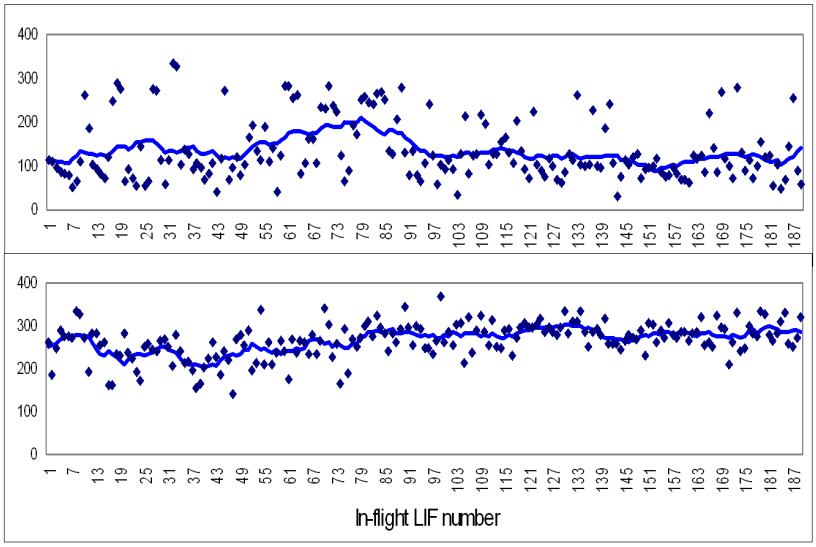

Figure 9: In-flight (top) and post-processed (bottom) DOM profiles of the Saugeen River (3 km distance). Dots correspond to data per single laser pulse, lines are averaged data.

While recorded profiles were smooth enough in the lake waters (Figure 7), the real-time processing of LIF spectra from river watershed causes problems due to several reasons. Firstly, the flight trajectory did not always precisely follow the river channels, and down-looking FLS-AU lidar recorded many LIF spectra from the river shores. Secondly, as the measurements were done in December, water-soaked melting snow observed on some river shores produced a Raman scattering signal, confusing the expert system and creating visual “noise” in measured profiles.

Additional processing was required to regularize the data. Figure 9 shows rough (in-flight) and regularized (by post-processing) profiles of DOM measured along the segment of the Saugeen River. The post-processing was based on the de-convolution of every measured LIF spectrum by using the pre-compiled LIF library and discrimination of the Raman signal to select the spots corresponding to the river channel. The discrimination level was defined statistically as 200 ADC reading units. As a result, the DOM distribution looks more regular (Figure 9 lower), while some points are missing and their location on the track is not homogeneous.

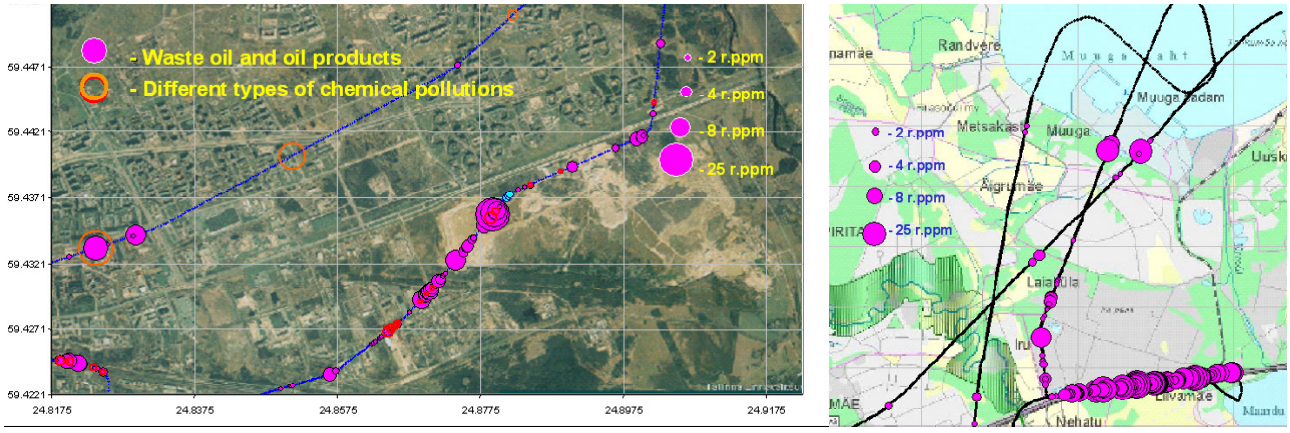

Figure 10: Location of ground pollution in industrial areas (left) and along railways (right) in the Tallinn city area.

The scanning lidar improves the observation of such targets as coastal zone, river channels, railways, roads and pipeline mains due to laser shots distribution inside the corridor. The experiments

aimed at detecting oil spills on water by FLS-AU lidar have indicated a need for the scanning mode of operation to improve the mapping of oil slicks with lidar.

In 2004-2005 the FLS-AM lidar was used in Estonia on board of a helicopter and tested at flight altitudes of up to 500 m to monitor sea and lake waters, industrial and port areas etc. Figure 10 shows an example of the oil and chemical pollutions location in the industrial area near the Tallinn city, dark lines show the flight path, and the bubbles display the findings.

Dense oil pollution marks in Figure 10 (right) correspond to the main railways transporting oil tanks, two polluted spots near the seashore correspond to the location of oil terminals. The oil pollution readings on ground were calibrated by equal fluorescence intensity of oil emulsion in water and shown in relative *ppm* (*rppm*).

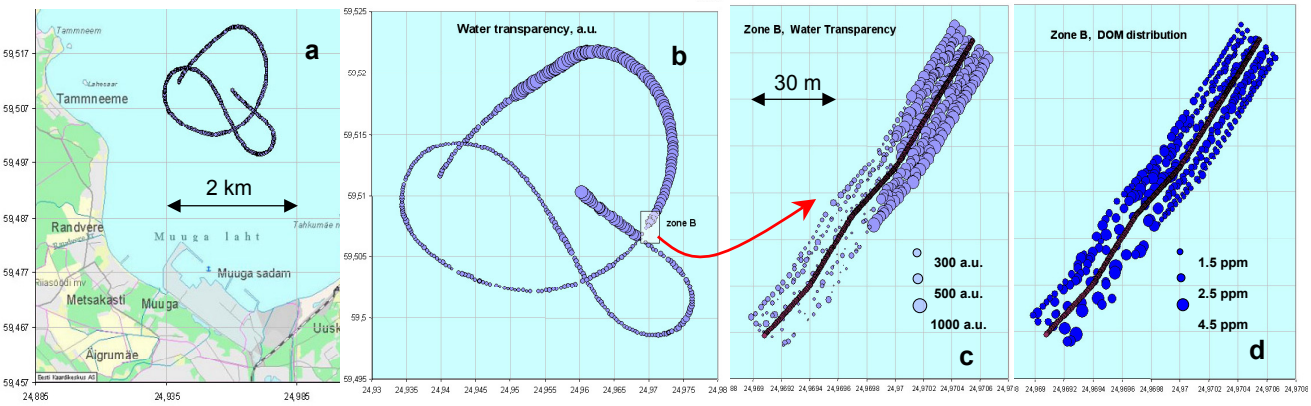

Figure 11: a) Flight path in the harbour bay (see Figure 10 for reference); b) profile of DOM distribution; c) detailed distribution of water transparency in zone B; d) detailed distribution of DOM in zone B (see Figure 10b for reference). The bubble size corresponds to the measured values.

Figure 11 demonstrates zoomed lidar profiles in the Tallinn harbour area. When flying over the trajectory according to Figure 11a the exact gradients of water transparency were detected in the central part of the bay where the navigation ways were crossed (Figure 11b). Figures 11c and d show the zoomed zone B to display the intensity of water Raman scattering (ADC readings) and the distribution of DOM measured at every position of the scanner (fluorescence intensities normalized to water Raman scattering).

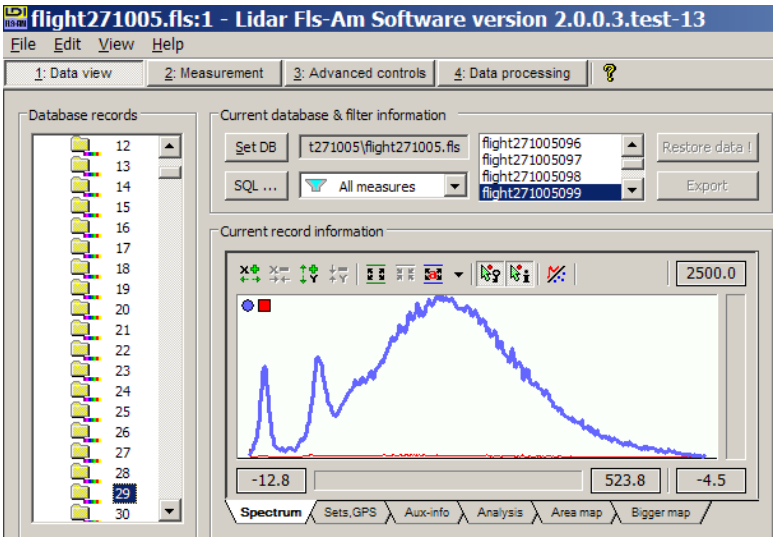

Figure 12: LIF spectrum of water in the Tallinn harbour area.

The gradient is clearly visible, and water transparency and DOM are not correlated. It indicates that lowering the transparency is rather caused by turbulence in the water column than by absorption due to higher DOM content. The first tests with scanning FLS-AM lidar have confirmed its good performances for a number of water and land applications. Fig.12 shows the operational screen of

FLS-AM software with the typical LIF spectrum of water per single laser pulse recorded in scanning mode (flight altitude 150 m).

In some cases the video frames synchronized in time were used to support post-processing especially when observing terrestrial targets.

Figure 13 shows the combined use of lidar- and video data when flying over the railway tanks. The bubbles' positions correspond to the laser shots on the ground, the size of the bubbles is proportional to the oil pollution level (*rppm*, see the scale in Figure 10). A value of 2 *rppm* was considered as a detection threshold. Bigger values were observed exactly on the oil tanks and sometimes around the rails. This confirmed the ability of lidar to monitor main lines, including oil pipelines.

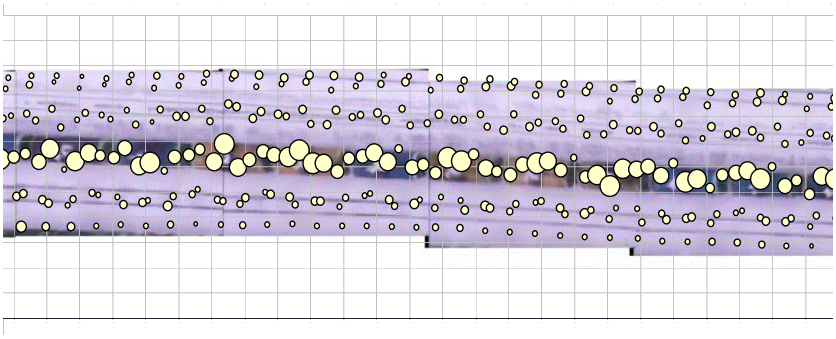

Figure 13: Combination of lidar and video data (120 m track).

CONCLUSIONS

The airborne surveillance projects carried out with the FLS-AU and FLS-AM lidars are already close to their operational use. A number of applications related to natural water quality and pollution detection have already been developed. In-flight data processing can provide a real-time targeting of ground activity (e.g. sampling) based on the findings. In case of a homogeneous distribution or trends of water quality parameters just a few ground samples are needed to quantify the remotely measured data. In more general cases, on-site SFS analysis of water samples at the points of interest (trend line fractures, pollution detected etc.) can be used to correct the LIF data calibration. A detailed laboratory analysis is necessary to verify the SFS data or to update the SFS library, but the total number of such analyses can be reduced significantly.

At the same time, real operational use requires more user needs to be answered. Some of the major demands have already been implemented in the new FLS-AM model. Pilot navigation screen with visualization of flight route and laser beam positions allows the lidar to be targeted easily according to the surveillance planning. The scanning mode of operation gives more flexibility to the pilot in doing necessary manoeuvers still keeping the target observed. The in-flight created short report on findings gives the benefit of in-time directing the ground activity, e.g. in case of pollution. Multi-wavelength excitation will bring more operational benefits for certain applications, such as the detection of submersed oil pollution (14), quantitative mapping of thicker oil films (9), simultaneous measuring of phytoplankton and DOM for eutrophication detection etc.

Some other issues are in the focus of running developments at LDI. First of all, the huge data volume collected in a few-hours' flight requires optimal data processing and management, both in-flight and in the post-processing mode. The real-time operational expert system must be capable of directing the ground activity according to the Multi-tier Environmental Assessment model with minimal time delay in reporting the coordinates and describing the findings. It requires further enhancement of the expert system algorithms in order to make them easily adjustable according to the flight mission. We consider an open data interface as a most promising model of lidar data management, providing the lidar data stream in a format compatible with the prevalent GIS software will facilitate the integration of these data into multi-layer maps which contain also additional information from other sensors.

ACKNOWLEDGEMENTS

The authors would like to thank the Ontario Ministry of Environment and River Conservation Authorities for the partnership in the project with FLS-AU lidar in Canada, Golder Associates for GIS data integration, and Estonian Air Forces for the cooperation in the airborne surveys in Estonia with FLS-AM lidars. The development of the FLS-AM lidar has been supported by Enterprise Estonia.

REFERENCES

1 Reuter R., H Wang, R Willkomm, K Loquay, T Hengstermann, and A Braun, 1995. A laser fluorosensor for maritime surveillance: Experimental results. EARSeL Advances in Remote Sensing, 3(3): 152-169

2 Zielinski O, R Andrews, J Göbel, M Hanslik, T Hunsänger & R Reuter, 2001. Operational Airborne Hydrographic Laser Fluorosensing. EARSeL eProceedings,1: 53-60

3 Brown C E, M F Fingas & J An, 2001. Laser Fluorosensors: A Survey of Applications and Developments of a Versatile Sensor. In: Proceedings of the Twenty-Fourth Arctic and Marine Oil Spill Program Technical Seminar (Environment Canada, Ottawa, ON) 485-493

4 Babichenko S, A Dudelzak & L Poryvkina, 2000. Lidar application in airborne monitoring of eutrophication and chemical pollution. In: Proceedings of the VI International Conference Remote Sensing for Marine and Coastal Environments (Charleston, SC) 2: 377-383

5 Chekaljuk A M, A A Demidov, V V Fadeev & M Yu Gorbunov, 1995. Lidar monitoring of phytoplankton and organic matter in the inner seas of Europe. EARSeL Advances in Remote Sensing, 3: 131-139

6 Barbini R, F Colao, R Fantoni, A Palucci & S Ribezzo, 1995. The ENEA lidar fluorosensor: results ob vegetation health. EARSeL Advances in Remote Sensing, 3: 215-219

7 Babichenko S, A Dudelzak & L Poryvkina, 2002. FLS-Lidar application in monitoring of marine and coastal environment. In: Lidar Remote Sensing for Industry and Environment Monitoring III, edited by U N Singh, T Itabe & Z Liu. Proceedings of SPIE, 4893: 456-464

8 Report on LDI3 airborne survey of three Great Lakes and associated watersheds conducted in December of 2003 in Southern Ontario, 2004 (Laser Diagnostic Instruments International Inc.) Publication 04-2004, 56 pp.

9 Lennon M, S Babichenko, N Thomas, V Mariette, G Mercier, and A Lisin, 2005. Detection and mapping of oil slicks in the sea by combined use of hyperspectral imagery and laser induced fluorescence. EARSeL eProceedings, 5(1)

10 Babichenko S, A Dudelzak & L Poryvkina, 2003. Laser remote sensing of coastal and terrestrial pollution by FLS-Lidar. EARSeL eProceedings, 3(1): 1-8

11 Babichenko S, A Leeben, L Poryvkina, E Rull & S Lapimaa, 2000. Spectral characterization of terrestrial and coastal waters in Estonia. Oil Shale, 17(2): 129-140

12 Babichenko S, L Poryvkina, Y Orlov, I Persiatsev & S Rebrik, 1998. Fluorescent Signatures in Environmental Analysis. The Encyclopedia of Environmental Analysis and Remediation (John Wiley & Sons Inc., New York) 1787-1791

13 Babichenko S, A Leeben, L Poryvkina, R Wagt & F Vos, 2000. Fluorescent screening of phytoplankton and organic compounds in sea water. Journal of Environmental Monitoring, 2(4): 378-383

14 Heavy Oil Detection with Laser Fluorometers, 2005. The Ohmsett Gazette (MAR Inc.) 6-7